iJRASET
International Journal For Research in
Applied Science and Engineering Technology

INTERNATIONAL JOURNAL
FOR RESEARCH
IN APPLIED SCIENCE & ENGINEERING TECHNOLOGY

**Volume:** 11 **Issue:** V **Month of publication:** May 2023

**DOI:** https://doi.org/10.22214/ijraset.2023.51824

International Journal for Research in Applied Science & Engineering Technology (IJRASET)
*ISSN: 2321-9653; IC Value: 45.98; SJ Impact Factor: 7.538*
*Volume 11 Issue V May 2023- Available at www.ijraset.com*

# Development of $SnO_2$: Ag Nanoparticle as an Affordable Catalyst for the Degradation of Gentian Violet Dye

A. Mubeenabanu[1], A. Bismibanu[2], T. Veemaraj[3]
*[1]Department of Chemistry, Ayya Nadar Janaki Ammal College (Autonomous), Sivakasi*
*[2]Department of Physics, Ayya Nadar Janaki Ammal College (Autonomous), Sivakasi*
*[3]Department of Chemistry, Ayya Nadar Janaki Ammal College (Autonomous), Sivakasi*

***Abstract:** An effective visible catalyst ($SnO_2$:Ag) was successfully synthesized using co-precipitation method for the decomposition of the dye Gentian Violet (GV). In addition to XRD, SEM and UV – Visible analysis, a variety of other physicochemical measurements were used to validate the as-prepared $SnO_2$:Ag nanoparticles. The phase identification of prepared sample is characterized by X – ray powder diffraction (XRD), which confirms the tetragonal rutile structure. The surface morphology is examined using a scanning electron microscope (SEM) and the optical absorption and the band gap value are calculated using the UV-visible spectrum. These results confirm the synthesis of nanoparticles by successive steps. A nanoparticles was demonstrated to be a superior catalyst for the degradation of GV dye when exposed to UV light. The photocatalytic activity studies are discussed using $SnO_2$:Ag nanoparticles. The degradation efficiency of the nanoparticle is 96 % towards the degradation of the GV dye.*

***Keywords:** Co-precipitation method, XRD, UV-Visible Spectroscopy, SEM and Gentian Violet dye.*

## I. INTRODUCTION

Now a day, the increase of industrial activities has intensified problems in environmental pollution and the deterioration of several ecosystems with the accumulation of pollutants, especially dyes. Effluents containing various dyes are discharged from various industrial processes. According to World Health Organization (WHO) the metals of the most immediate concern are effluents from various textile industries (cationic, anionic and neutral dyes), organic acids, heavy metals. Dyes may be found in wastewater discharges from the manufacture of pigments dyes and textile operations. The waste generated by the textile industry not only poses a threat to human health, but also poses a threat to the environment, so appropriate remedial technologies are needed [1–3]. In particular, organic dyes are highly stable and easily identifiable compounds in water, which can cause life-threatening problems. Therefore, various technologies such as adsorption, membrane filtration, chemical oxidation, biological digestion, electrochemical oxidation and advanced oxidation process (AOP) are widely used to remove organic pollutants in water. Compared with other methods, the AOP-based semiconductor photocatalytic decomposition process has been proven to be efficient and environmentally friendly. Among the most promising approaches, semiconductor-based photocatalysts have been recognized for their economic, environmentally friendly, and well-organized nature. In addition, semiconductor based photodegradation processes have attracted curiosity due to their harmlessness, effectiveness, and stability [[4, 5]. There are numerous metal oxide semiconductor materials in various shapes and structures that have proven effective in the degradation of organic dyes, including ZnO, $TiO_2$, CuO, and MgO. Compared to $TiO_2$, ZnO has a broad direct band gap (3.37 eV), high binding energy for excitation (60 meV), and excellent electrical, mechanical, and optical and photocatalytic properties. Ag doped with metal oxides can significantly improve the photocatalytic activity.

According to experimental calculations, $SnO_2$ is significant n-type semiconductors with a broad energy band gap (3.6 eV) among the metal oxides (ZnO, $TiO_2$, $WO_3$, $CeO_3$ and so on). It has a wide range of uses in gas sensors, optoelectronic devices, dye base solar cells, secondary lithium batteries, and catalysts due to its optical transparency in the visible area. The Sol-gel and microwave procedures, evaporative breakdown of solution [6], template-assisted growth [7], wet chemical synthesis [8], and gas-phase reaction [9, 10] are only a few of the many techniques used to create silver doped $SnO_2$ nanoparticles. For the synthesis of silver doped $SnO_2$ nanoparticles, we chose the chemical co-precipitation approach over the others because it allows us to easily regulate the structural and surface characteristics of the nanoparticles.

Transparent conducting oxides such as $SnO_2$ have a great technological potential related to the ideal combination of electrical and optical properties. Since they have found many applications in technology, the $SnO_2$-based systems are extensively studied. Particularly, for gas sensing materials the sensitivity is strongly dependent upon the crystallite size and shape, inasmuch as this property is influenced by the surface to volume ratio in $SnO_2$:Ag systems [11**]**.

### *A. Experimental Details*

Synthesis of Ag doped $SnO_2$

Nanoparticle samples of $SnO_2$: Ag were prepared by Co-precipitation method. The starting materials are Tin Chloride $SnCl_2$/$AgCl_2$ and Sodium hydroxide (NaOH). We dissolved 1M of $SnCl_2$in 100 ml $H_2O$ under heating and continuous stirring of 30 minutes. Then, various concentrations (x=1 and 3%) of silver nitrate [$AgNO_3$] were used for preparing the doped samples. Then sodium hydroxide (0.5 mol) was dissolved in 100 ml of distilled water and added drop wise to the stirring solution of Tin chloride and the mixture was stirred using magnetic Stirrer for 2 hours. The precipitate was filtered and annealed at 80° C. The dried sample was also calcined at 550° C.

## II. RESULT AND DISCUSSSIONS

### *A. Structural Properties*

Pure and Ag doped $SnO_2$ nanoparticles

Figure 1 revealed the crystal structure and phase of the $SnO_2$ and $SnO_2$:Ag were recorded by XRD analysis. The peaks at 2θ values at 26.1º, 33.2º, 37.4º and 51.2º can be associated with (110), (101), (200) and (211) respectively. Peaks can be ascribed to tetragonal rutile structure.

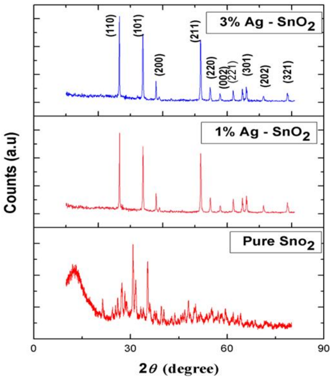

Figure 1 XRD for undoped and Ag doped $SnO_2$ for various concentrations (1% and 3%)

The lattice constant 'a' and 'c' of tetragonal rutile structure of $SnO_2$ can be calculated using the relation given below.

$$\frac{1}{d^2} = \frac{h^2+k^2}{a^2} + \frac{l^2}{c^2}$$

The peaks in the XRD spectrum correspond to those of the $SnO_2$ pattern [**12**] from the JCPDS data (powder diffraction file card no: 88-0287) having tetragonal rutile structure with lattice constants a=4.737Å, C=3.1864Å and a/c=1.4866. The a and c values obtained for Ag doped $SnO_2$ nanoparticles prepared in this work are a=4.6111,c=3.1864 and a/c= 1.2171.

Table 1 Peak position, crystallite size, the lattice parameter a, c and its ratio

| Sample | Ag doping wt% | 2θ values along (110) plane deg | Crystallite size D in (nm) | A (Å) | B (Å) | a/c |
|---|---|---|---|---|---|---|
| Pure $SnO_2$ | 0 | 26.9 | 45.2 | 4.6111 | 3.7884 | 1.2171 |
| | 1 | 26.6 | 41.3 | 4.7391 | 3.1886 | 1.4862 |
| | 3 | 26.5 | 38.1 | 4.7460 | 3.1907 | 1.4874 |

From XRD studies the crystallite size were in the range 38 to 45 nm and the crystallite size decrease with increasing Ag doping concentration it may be due to the small ionic radii of $Ag^+$ (0.115nm) when compared to $Sn^{2+}$ ion (0.118 nm) [13].

### *B. Optical Properties*

UV-Visible Spectra for Ag doped $SnO_2$ nanoparticles

The UV-Vis absorption spectroscopy has been carried out to understand the optical properties and electronic interaction of doped nanoparticles. In order to confirm the substitution of $Sn^{2+}$ by $Ag^{+}$ ions, the optical absorption spectra for $SnO_2$:Ag nanoparticles were measured at room temperature as shown in Figure 2.

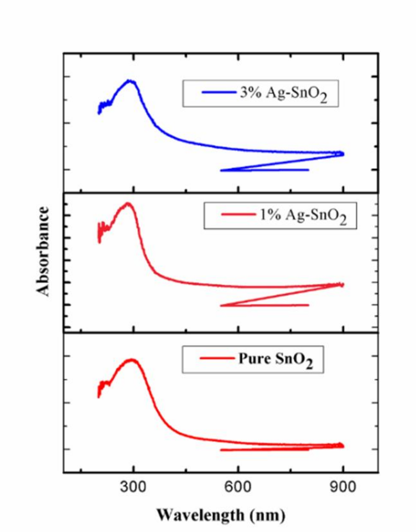

Fig. 2 UV absorbance spectra for undoped and Ag doped $SnO_2$ for various concentration (1 and 3%)

The absorption spectrum of pure $SnO_2$ shows the sharp absorption peak at 299 nm (3.27ev). The increase in band gap is mainly due to the incorporation of Ag atoms in $SnO_2$.The band gap spectra of Ag doped $SnO_2$ in various concentrations of 1 wt % and 3 wt % Ag doped $SnO_2$ samples were shown in Figure 2.1, 2.2 and 2.3.

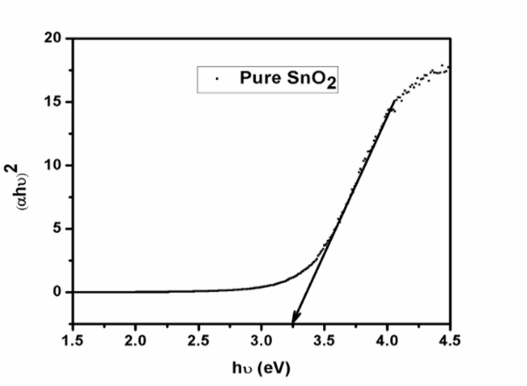

Fig. 2.1 Band gap diagram for undoped $SnO_2$

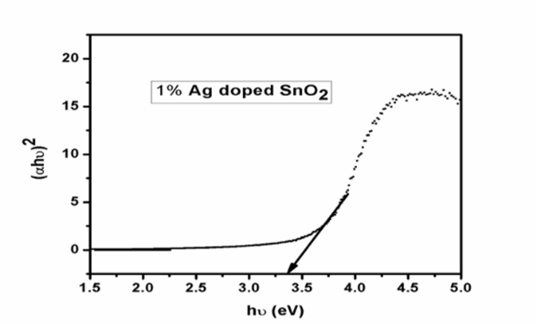

Fig. 2.2 Band gap diagram for 1% Ag doped $SnO_2$

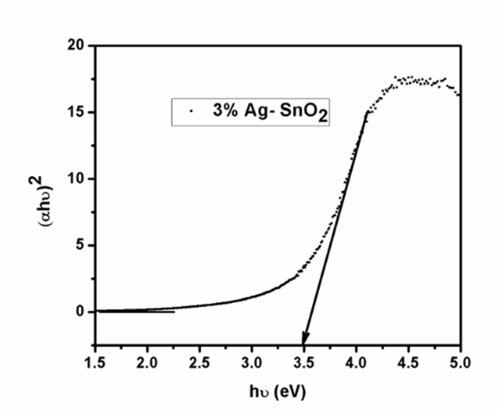

Fig. 2.3 Band gap diagram for 3% Ag doped $SnO_2$

The above plot exhibited a fundamental absorption edges at 286 nm and 283 nm corresponds to 3.39 ev and 3.49 ev respectively. The resultant values confirm that the well blue shift was occurred by increasing the dopant concentration due to the high incorporation of Ag within $SnO_2$, which makes the material as a vastly doped $SnO_2$:Ag nanoparticle [**14**].

Table 2 UV Visible absorption data for the $SnO_2$ and $SnO_2$:Ag nanoparticles

| Sample | Ag doping (wt %) | λ (nm) | Band gap (eV) |
|---|---|---|---|
| Pure $SnO_2$ | 0 | 299 | 3.27 |
| | 1 | 286 | 3.39 |
| | 3 | 283 | 3.49 |

*C. Morphological Properties*

SEM for pure $SnO_2$ and Ag doped $SnO_2$

The surface morphology of as-prepared pure $SnO_2$ and $SnO_2$:Ag was analyzed by SEM spectroscopic analysis was shown in Figure 3.1, 3.2, and 3.3.

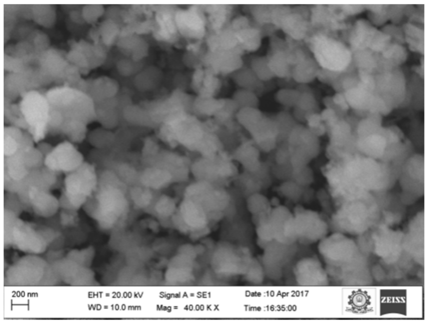

Fig. 3.1 SEM image for pure $SnO_2$

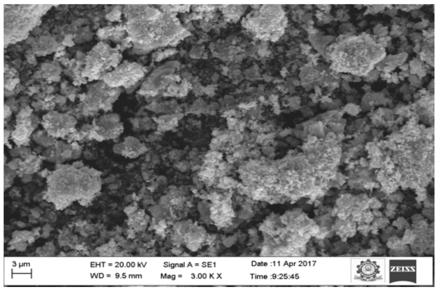

Fig. 3.2 SEM image for 1% Ag-$SnO_2$

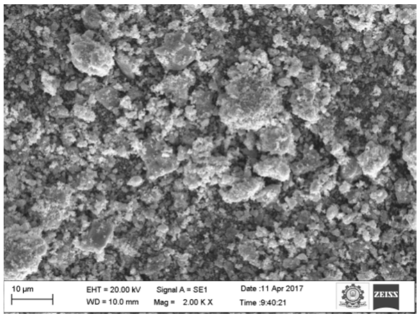

Fig. 3.3 SEM images for 3% Ag-$SnO_2$

The above figures shows the SEM images of Ag doped $SnO_2$ with different concentration of 1wt% and 3wt% respectively. The Pure $SnO_2$ shows the tetragonal shape. This tetragonal shape is changed to spherical for various doping concentration of Ag (1 wt% and 3 wt%). This indicates that the Ag doping into $SnO_2$ can change the surface character of the primary nanoparticles, which was deduced to be from the effects of the diffusion of $Ag^+$ into the $SnO_2$ lattice, and the formation of Ag-O-Sn bond on the surface of the doped samples were confirmed **[15, 16].**

### *D. Applications of Nanomaterials*

Photocatalytic activity

It is important from mechanistic and application point of view to study the dependence of substrate concentration on the photocatalytic degradation rate**.** Photocatalytic activity studies confirmed that when increase the dose of the catalyst with increase the percentage of removal (%R) and Ag-doped nanoparticles enhanced the rate of degradation of Gentian Violet (GV) dyes. In the absence of catalyst, pure $SnO_2$ which has the lower efficiency (0.1g in 58% and 0.5g in 65% removal of dye). In the presence of catalyst, Percentage removal of dyes increased with the increased with increase in contact time and dose of catalyst. Amount of dyes adsorbed increases with the decrease in particle size of catalyst. This results shows that the efficiency of catalyst increases upto 96.00 % for the removal of GV dye **[17-21].**

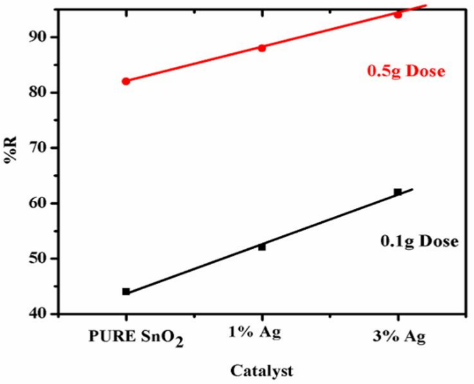

Fig 5. Photodegradation of GV dye on pure $SnO_2$ and Ag doped $SnO_{2.}$

## III. CONCLUSION

A novel $SnO_2$ nanomaterial are well dispersed on Ag nanoparticle was demonstrated by a fruitful coprecipitation method. As prepared nanoparticle was characterized thoroughly by adopting various analytical techniques. This nanoparticle could be used as economically very feasible catalyst alternative to other commercially available catalyst for the cost effective treatment of effluents, especially for the removal of industrial dyes in general and Gentian Violet in particular using co-precipitation method. The XRD pattern of the Ag doped $SnO_2$ nanoparticles were indexed to the tetragonal structure with average crystallite sizes in the range 45 -38 nm. The UV- Visible spectral studies concluded that the optical band gap of the Ag doped $SnO_2$ were found to be 3.27 eV, 3.39 eV and 3.49eV. The SEM images revealed that the Pure $SnO_2$ shows the tetragonal shape. This tetragonal shape is changed to spherical for various doping concentration of Ag. Photocatalytic activity studies confirmed that when increase the dose of the catalyst with increase the percentage of removal (%R) and Ag-doped nanoparticles enhanced the rate of degradation of dyes.

## IV. ACKNOWLEDGEMENTS

The authors thank the Management and Principal of ANJA College, Sivakasi, for providing facilities and encouragement. The authors also thank the TNSCST, Chennai, for financial assistance under Student Project scheme.

## REFERENCES

[1] Subramanyam, N., Sreelekha, G., Murali, G., Giribabu, G. and R.P. Vijayalakshmi, (2014) "Influence of Co Doping on structural and Optical properties of $SnO_2$ Nanoparticles", International Journal of Chemistry, **6,** 2051-2053.

[2] Bouaine, A., Brihi, N., Schmerber, G., Ulhahq Bouillet, C., Coils, and S., Dinia, A., (2007) "Structural, Optical and Magnetic Propeties of Co-doped $SnO_2$ powders synthesized by the co-precipitation method", The Journal of Physical Chemistry C, **111,** 2924-2928.

[3] Yu, A.S. and French, R. (2002) "Coating of multi-walled carbon nanotube with $SnO_2$ films controlled Thickness and its application for Li-ion battery", J. Power Sources., **104**, 97-102.

[4] Lu, C.H. and Yeh, C.H, (2000) "Influence of hydrothermal conditions on the morphology and particle size of zinc oxide powder", Ceramics International, **26**, 351-357.

[5] Milliron, D.J., Hughes, S.M., Cui, Y., Manna, L., Li, J., Wang, L.W., and Alivisatos, A.P., (2004) "Colloidal nanocrystal heterostructures with linear and branched topology" Nature, **430,** 190-195.

[6] Neves, M.C., Trindade, T., Timmons, A.M.B. and Pedrosa de Jesus, J.D., (2001) "Synthetic hollow zinc oxide microparticles", Materials research bulletin, **36,** 1099-1108.

[7] Ni, Y.H., Wei, X.W., Ma, X. and Hong, J.M., (2005) "CTAB assisted one-pot hydrothermal synthesis of columnar hexagonal-shaped ZnO crystals", Journal of crystal growth, **283,** 48-56.

[8] Pan, Z. W., Dai, Z. R., & Wang, Z. L. (2001) "Nanobelts of semiconducting oxides", Science, **291 (5510**), 1947-1949.

[9] Rodriguez, J.A., Jirsak, T., Dvorak, J., Sambasivan, S. and Fischer, D.J., (2000) "Reaction of $NO_2$ with Zn and ZnO: Photoemission, XANES, and Density Functional Studies on the Formation of $NO_3$", The Journal of Physical Chemistry B, **104**, 319 -328.

[10] Thakare, M.G., Dighavkar, C.G., Aher, J.S., (2016) "Effect of Pt doping ZnO nanoparticles" International Journal of Recent Trends in Engineering and Research, **2**, 1-5.

[11] Aragon, F.H., Coaquira, J.A.H., Villengas- Lelovsky, L., da Silva, S.W., Cesar, D.F., Nagamine, L.C.C., Cohen, R. and Morais, P.C., (2015) "Evolution of the doping regimes in the Al-doped $SnO_2$ nanoparticles prepared by polymer precursor method". Journal of Physics: Condensed Matter, **27**, 1-7.

[12] Salam Amir, Y. and Jenan Mohamed, A., (2013), "Structural, Morphological and Optical Characterization of SnO2: F thin films prepared by Chemical spray Pyrolysis", International Letters of Chemistry, Physics and Astronomy, **13**, 90-102.

[13] Thakare, M.G., Dighavkar, C.G., and Aher, J.S., (2016) "Effect of Pt doping on ZnO nanoparticles", International Letters of Chemistry, Physics and Astronomy, **2**, 1-5.

[14] Jianlong, R., Xuechong, Shi, Y., Yu, G., Yuanyuan, T. and Zhonghua, W., (2013) "Synthesis and structural characterization of ZnO doped with Co" Jounal of Alloys and Compounds, **558**, 212-221.

[15] Aragon, H., Coaquira, J.A.H., Villegas Lelovsky, L., da Silva, S.W., Cesar, D.F., Nagamine, L.C.C.M., Cohen, R., Menendez-Proupinand, E., Morais, P.C., (2015) "Evolution of the doping regimes in the Al-doped $SnO_2$ nanoparticles prepared by a polymer precursor method, Journal of Physics: Condensed Matter, **27**, 1-7.

[16] Vadivel, M., Ramesh Babu, R. and Ramamurthi, K. (2015) "Studies on the structural, optical and magnetic properties of Al doped ZnO nanoparticles". International Journal of Chem Tech Research, **7**, 1206-1211.

[17] Xu, L., Au, Y., Pelligra, C., Chen, C., Jin, L., Huang, H., Sithambaram, S., Aindow, M., Joeshon, R., and Suib, S.L., (2009), "ZnO with different morphologies synthesized by solvothermal methods for enhanced photocatalytic activity", Chemistry of Materials, **21**, 2875-2885.

[18] Mc Mullan, G., Meehan, C., Conneely, A., Kirby, N., Robinson, T., Nigam, P., Banat, I.M., Marchant, R. and Smyth, W.F., (2001) "Microbial decolourisation and degradation of textiles dyes", Application Microbial Biotechnolog, **56**, 81-87.

[19] Kumar, V., Wati, L., Nigam, P., Banat, I.M., Yadav, B.S., Singh, D. and Marchant, R., (1998), Decolourization and "biodegradation of anaerobically digested sugarcane molasses spent wash effluent from biomethanation plants by white-rot fungi", Process Biochemistry, **33**, 83-88.

[20] Ravelli, D., Dondi, D., Fagnonia, M. and Albini, A., (2009) "Photocatalysis: A multi-faceted concept for green chemistry", Chemical Society Reviews, **38,** 1999-2011.

[21] Jagessar, R.C., Mars, A. and Gomes, G., (2008) "Selective Antimicrobial properties of Phyllanthusacidus leaf extract against Candida albicans, Escherichia coliand Staphylococcus aureususing Stokes Disc diffusion, Well diffusion, Streakplate and a dilution method", Nature and Science, **6(2)**, 24-38.

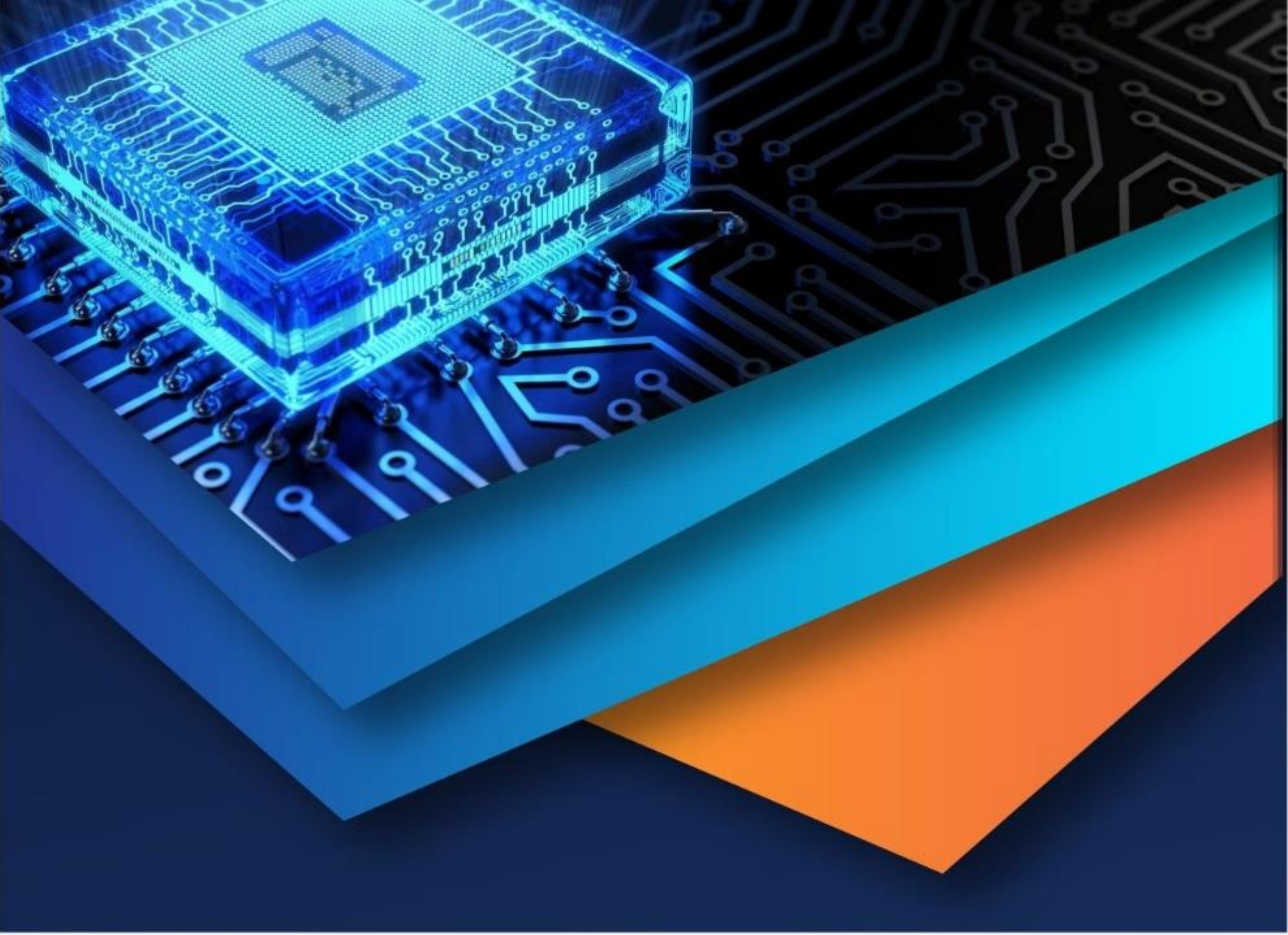

# INTERNATIONAL JOURNAL FOR RESEARCH

IN APPLIED SCIENCE & ENGINEERING TECHNOLOGY